Research Square

Preprints are preliminary reports that have not undergone peer review.
They should not be considered conclusive, used to inform clinical practice,
or referenced by the media as validated information.

Development of Periodically Poled Lithium Niobate Waveguides for 780 nm Femtosecond Lasers

Xiaohu Xu
Huazhong University of Science and Technology
Kang Zou
zoukang@cssc717.com
Huazhong Institute of Electro-Optic
Shuo Zhang
Huazhong Institute of Electro-Optic
Shuai Yuan
Wuhan ANPI Optoelectronics Company Ltd
An Pan
Wuhan ANPI Optoelectronics Company Ltd
Ke Li
Huazhong Institute of Electro-Optic
Zhiqiang Qi
Huazhong Institute of Electro-Optic

Research Article

Keywords: femtosecond laser, periodically poled lithium niobate, second harmonic generation, ridge waveguide, nonlinear frequency conversion

Posted Date: November 20th, 2026

DOI: https://doi.org/10.21203/rs.3.rs-11633746/v1

License: This work is licensed under a Creative Commons Attribution 4.0 International License.
Read Full License

Additional Declarations: No competing interests reported.

Development of Periodically Poled Lithium Niobate Waveguides for 780 nm Femtosecond Lasers

Xu Xiaohu[1], Zou Kang[2*] , Zhang shuo[2] , Yuan Shuai[3] , Pan An[3] , Li Ke[2] and Qi Zhiqiang[2]
（1 Huazhong University of Science and Technology, Wuhan 430074, Hubei, China;
2 Huazhong Institute of Electro-Optic, Wuhan 430223, Hubei, China;
3 Wuhan ANPI Optoelectronics Company Ltd, Wuhan, 430200, Hubei, China）
Corresponding authors：Zou Kang, zoukang@cssc717.com.

Abstract: 780 nm femtosecond lasers are important for laser processing, multiphoton imaging, terahertz generation, and quantum-entangled light sources. This study presents the fabrication of periodically poled lithium niobate (PPLN) waveguide chips and packaged devices for these applications. By optimizing chip design, periodic electrode fabrication, domain inversion, waveguide etching, end-face polishing, and antireflection coating, high-quality PPLN ridge waveguides of different lengths were fabricated. A stable, plug-and-play device with fiber-coupled input and free-space second-harmonic output was developed. Under pump conditions of 40.0 mW average power, 50 fs pulse duration, and 80 MHz repetition rate, the device generated 17.2 mW at 780 nm, achieving a conversion efficiency of 43.0%, significantly exceeding that of conventional bulk PPLN. When the fundamental-wave average input power increased to 80.0 mW, the pulse duration broadened to 100 fs. The measured second-harmonic power was 30.1 mW, corresponding to a conversion efficiency of 37.6%. The results indicate that increasing fundamental-wave average power leads to pulse broadening and consequently reduces conversion efficiency. Under both input conditions, the output power stability was better than 0.2% RMS over 2 hours. These waveguides combine efficient nonlinear frequency conversion with high power-handling capacity, making them suitable for high-power, high-efficiency 780 nm femtosecond second-harmonic generation. This work advances the investigation of nonlinear properties in thin-film lithium niobate and the engineering application of femtosecond frequency-doubling waveguides.

Keywords: femtosecond laser; periodically poled lithium niobate; second harmonic generation; ridge waveguide; nonlinear frequency conversion

1 Introduction

780nm femtosecond lasers play a critical role in numerous fields, including laser processing [1], multiphoton imaging [2], terahertz wave generation [3], and quantum entangled photon pair generation [4]. Traditional titanium-sapphire lasers can directly generate 780 nm femtosecond pulses [5]; however, they suffer from inherent drawbacks such as structural complexity, prohibitive cost, and large physical footprint. Frequency doubling of femtosecond lasers at the 1560 nm telecommunications band using periodically poled lithium niobate (PPLN) waveguides has emerged as the mainstream technical approach for achieving 780 nm femtosecond laser output [6]. The key advantage of this approach lies in the mature fiber laser technology and low-loss fiber-

optic components available in the 1560 nm wavelength regime; through highly efficient frequency conversion in PPLN waveguides, high-power, high-beam-quality 780 nm femtosecond laser output can be obtained [7]. Currently, nonlinear frequency conversion is predominantly performed using bulk nonlinear crystals, which require free-space coupling into the crystal, limiting conversion efficiency. Furthermore, optical path coupling necessitates precise alignment and is sensitive to environmental disturbances, making it difficult to realize full-fiber integration. In this paper, a periodically poled ridge waveguide structure is fabricated on a thin-film lithium niobate platform, confining the optical field within a micrometer-scale region and significantly enhancing the optical power density and nonlinear interaction strength within a shorter device length. The fabricated PPLN waveguide is directly coupled to the optical fiber, exhibiting low loss, a compact structure, and stable performance, successfully realizing highly integrated and efficient frequency doubling for 780 nm femtosecond lasers.

2 Basic Principles and Experimental Setup

2.1 Quasi-Phase Matching Technology

Nonlinear frequency conversion technology represents an important technique in modern optics, which exploits the nonlinear optical properties of materials to achieve conversion between different optical frequencies [8] and extending the range of laser wavelengths. For second-order nonlinear processes, electromagnetic waves must satisfy energy and momentum conservation conditions:

$$\omega_1 + \omega_2 = \omega_3 \qquad (1)$$

$$k_1 + k_2 = k_3 \qquad (2)$$

Where ω_i represents the angular frequency of the optical field, and k_i represents the wave vector of the optical field.

Second-order nonlinear processes include second harmonic generation, sum frequency generation, difference frequency generation, optical parametric amplification, and optical parametric oscillation. To achieve efficient nonlinear frequency conversion, phase matching techniques must be employed to enhance the nonlinear frequency conversion efficiency, as illustrated in figure 1.

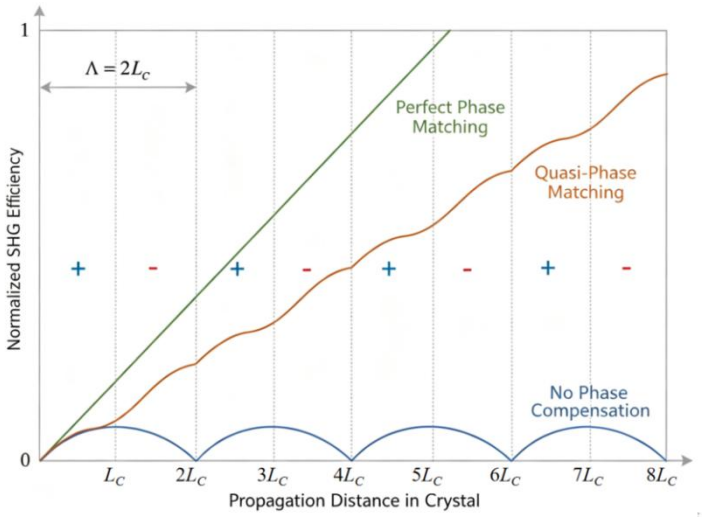


Figure 1 Comparison of perfect phase matching, quasi-phase matching, and phase mismatch efficiencies

To overcome the dispersion problem arising from the propagation of light at different frequencies in nonlinear media, the commonly adopted approaches are as follows:

1) Angle phase matching: The phase-matching relationship among the interacting optical waves is tuned by exploiting the dependence of the refractive index on the incident angle in birefringent crystals.
2) Temperature phase matching: Phase matching is achieved by controlling the crystal temperature, taking advantage of the temperature-dependent refractive index of nonlinear crystals.
3) Quasi-Phase Matching (QPM): Signal enhancement is obtained by periodically modulating the sign of the nonlinear susceptibility to compensate for the phase mismatch.

PPLN waveguides leverage QPM technology combined with low-loss waveguide fabrication techniques on lithium niobate on insulator (LNOI) to realize periodic domain inversion structures in micrometer-scale optical waveguides. A comparison of the domain engineering fabrication processes via the external electric field poling method between bulk PPLN and thin-film PPLN is presented in figure 2.

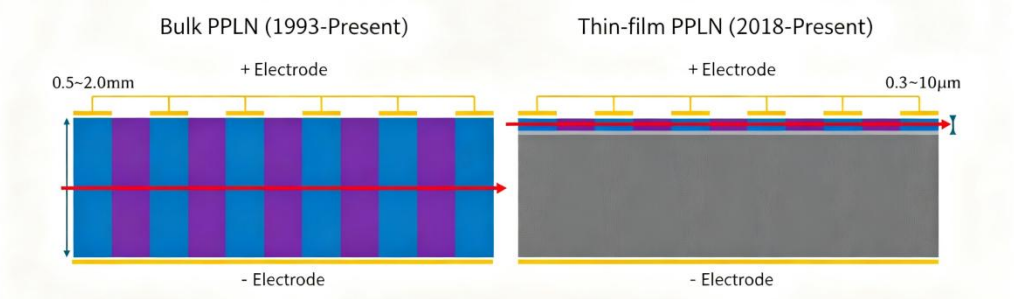


Figure 2 Comparison diagram of PPLN process between bulk material and thin film

Bulk materials typically have thicknesses of several hundred micrometers, leading to non-uniform longitudinal domain fabrication and significant poling difficulty. In contrast, thin-film materials are only a few micrometers in thickness, which enables the realization of high-quality, uniform domain structures via the direct external electric

field poling method. Combined with direct fiber-to-waveguide coupling integration, this approach effectively enhances the nonlinear interaction between the fundamental and second harmonic waves, improves frequency conversion efficiency, and simultaneously enables stable and reliable system integration.

2.2 Principle of Femtosecond Pulse Second Harmonic Generation

Frequency doubling, also known as second harmonic generation (SHG), is a second-order nonlinear optical process. Lithium niobate ($LiNbO_3$) exhibits a large second-order nonlinear coefficient. By periodically modulating the second-order susceptibility, the fundamental and second-harmonic waves can be kept phase-synchronous during propagation through the crystal, thereby effectively enhancing the conversion efficiency. Under the small-signal approximation, the SHG conversion efficiency can be expressed as:

$$\eta=\frac{2\omega^2 d_{eff}^2 L^2 P_\omega(0)}{\varepsilon_0 c^3 n_{2\omega} n_\omega^2 A_{eff}} sin\, c^2\left(\frac{\triangle kL}{2}\right) \qquad (3)$$

where $P_\omega(0)$ is the fundamental power, and A_{eff} is the effective cross-sectional area of the fundamental mode in the crystal.

Equation (3) shows that the SHG efficiency is proportional to the square of the crystal length, the square of the effective nonlinear coefficient, and the fundamental intensity, and simultaneously governed by the $sin\, c^2(\triangle kL/2)$ function. When $\triangle kL=\pi$, the SHG intensity reaches its maximum.

Owing to the high energy density of femtosecond pulses and the strong two-dimensional optical confinement provided by periodically poled lithium niobate (PPLN) waveguides, the frequency conversion efficiency can be driven to elevated levels. In this regime, the small-signal (non-depletion) approximation no longer holds, and the depletion of the fundamental wave during propagation must be taken into account [9]. Under such conditions, the SHG conversion efficiency is given by:

$$\eta=\frac{I_{2\omega}(L)}{I_\omega(0)}=\tanh^2\left(\frac{L}{L_{SHG}}\right) \qquad (4)$$

Where $L_{SHG}=(2\omega d_{eff}E_1(0)/cn)^{-1}$ is the effective SHG length. From this equation, it can be seen that during femtosecond-pulse second-harmonic generation, the dependence of the conversion efficiency on the crystal length is non-monotonic, indicating the existence of an optimal effective SHG length.

2.3 Numerical Simulation of Femtosecond Pulses

Femtosecond pulse lasers compress the laser energy into a temporal width on the order of femtoseconds, implying an extremely high peak power density within an ultrashort time window. When such a laser passes through a nonlinear crystal, a high frequency conversion efficiency can be maintained even over a relatively short interaction length; however, it is ultimately constrained by nonlinear effects such as group velocity dispersion (GVD), self-phase modulation (SPM), and cross-phase modulation (XPM).

Under the slowly varying amplitude approximation, the femtosecond-pulse SHG process can be described by the following coupled-wave equations when waveguide

loss is neglected [10-11]:

$$\frac{\partial E_1}{\partial z}-\frac{i}{2}\beta_{21}\frac{\partial^2 E_1}{\partial \tau^2}=-i\kappa d_{eff}E_2E_1^*e^{-iV\!kz}$$
$$-i\frac{n_2k_1}{n_{01}}(|E_1|^2+2|E_2|^2)E_1 \quad (5)$$

$$\frac{\partial E_2}{\partial z}+(\frac{1}{v_2}-\frac{1}{v_1})\frac{\partial E_2}{\partial \tau}-\frac{i}{2}\beta_{22}\frac{\partial^2 E_2}{\partial \tau^2}=$$
$$-i\kappa d_{eff}E_1^2e^{-i\Delta kz}-i\frac{n_2k_2}{n_{02}}(|E_2|^2+2|E_1|^2)E_2 \quad (6)$$

Where E_i is the field amplitude, $v_i$is the group velocity, β_{2i} is the GVD coefficient, n_{0i} is the refractive index, k_i is the wave vector, n_2 is the third-order nonlinear refractive index, τ is the coupling coefficient, S_{eff} is the effective waveguide area, $\Delta k=k_2-k_1-2\pi/\Lambda$ is the phase mismatch, and Λ is the phase matching period of the PPLN. Letting $\tau=t-z/v_1$, the fundamental pulse width is $L_w=T_0/(1/v_1-1/v_2)$ (where T_0 is the full width at half maximum of the fundamental intensity).

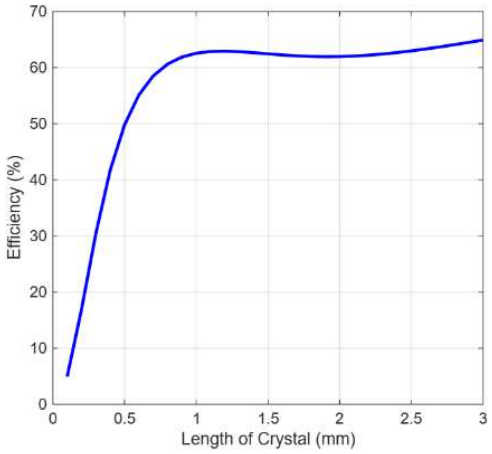
The nonlinear partial differential equations (5) and (6) are solved numerically using the split-step Fourier method. The equations are decomposed into a linear dispersion term and a nonlinear effect term, and the fourth-order Runge-Kutta method is employed for the numerical integration. The relationship between the SHG conversion efficiency and the crystal length is calculated for a fundamental wave with an average input power of 40.0 mW, a pulse duration of 100 fs, and a repetition rate of 80 MHz. The SHG parameters are obtained from waveguide simulations using Lumerical software, as listed in Table 1.

Table 1 SHG Simulation Parameters of Waveguide

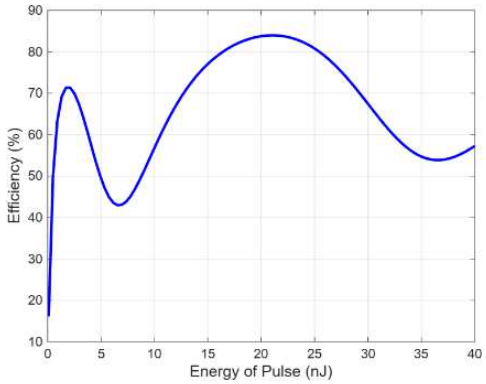
Parameters	Value
T_0	100fs
$1/v_1-1/v_2$	282ps/m
n_{01}	2.1275
n_{02}	2.1684
β_{21}	-672ps^2/km
β_{22}	336ps^2/km
S_{eff}	66μm^2
d_{eff}	11.8pm/V
n_2	0.1nm^2/W
Δk	2mm^{-1}
E_{pulse}	0.5nJ

The first step of the algorithm is frequency-domain processing of the linear part, where dispersion and group-velocity mismatch (GVM) effects are handled in Fourier space. The second step is time-domain processing of the nonlinear part, where nonlinear

coupling effects are treated in the temporal domain. The third step is iterative propagation: the crystal is divided into multiple short segments, with the linear and nonlinear steps applied alternately in each segment. A fourth-order Runge–Kutta (RK4) method is then employed to improve the computational accuracy of the nonlinear part. The simulation results are shown in Figure 3 below.



(a) Dependence of femtosecond SHG conversion efficiency on crystal length



(b) Dependence of femtosecond SHG conversion efficiency on pulse energy

Figure 3 Femtosecond pulse numerical simulation results: (a) dependence of conversion efficiency on crystal length, (b) dependence of conversion efficiency on incident single-pulse energy

Figure 3(a) shows that the femtosecond SHG conversion efficiency varies non-monotonically with increasing crystal length, reaching maxima or minima at specific lengths. The positions of these extrema are related to the single-pulse energy of the femtosecond laser. Figure 3(b) indicates that the single pulse energy also affects the effective nonlinear conversion efficiency of the femtosecond SHG process. The conversion efficiency displays a nonlinear dependence on both the crystal length and the input single-pulse energy. Therefore, both the crystal length and the fundamental-wave input conditions must be jointly considered in order to achieve high conversion efficiency or high output optical power.

It should be noted that, in actual experiments, the femtosecond pulses may significantly enhance the detrimental effect of GVM on the phase-matching condition.. The SPM and XPM arising from the Kerr nonlinearity introduce additional intensity-dependent phases during propagation, which also exert a certain suppressive effect on

the SHG conversion efficiency. Consequently, β_{2i} will increase, leading to larger optimal crystal lengths in simulations; the optimal crystal length is expected to lie in the range of 0.5-2mm. For a given repetition rate, a narrower pulse width corresponds to a higher single pulse energy, leading to greater SHG efficiency until saturation is reached.

3 Experimental Results and Analysis

3.1 Fabrication of PPLN Waveguide Chips for 780 nm Femtosecond Lasers

The fabrication of PPLN waveguide chips for 780 nm femtosecond lasers generally involves six steps: chip design, electrode fabrication, poling, etching, dicing and polishing, and coating.To determine the optimal crystal length, chips with four different lengths (0.50 mm, 1.00 mm, 1.50 mm, and 2.00 mm) are fabricated. The detailed procedures for chip design, wafer processing, and testing are as follows:

⑴ **Design:** The periodic electrode structure was designed using L-Edit software. Periodic electrodes were fabricated on the +Z face of a 10-μm-thick thin-film lithium niobate (TFLN) layer, with a 500-μm-thick silicon wafer serving as the substrate and a 2-μm-thick SiO_2 (buried oxide) layer in between. The chip dimensions are 0.50 mm (L) × 3.40 mm (W) × 0.51 mm (H), with four variants differing only in length. Each chip contains three channels, labeled A, B, and C, corresponding to designed poling periods of 18.8 μm, 19.0 μm, and 19.2 μm, respectively.

⑵ **Electrode Fabrication:** The electrode pattern on the photomask was transferred onto the wafer using a photolithography process. Subsequently, a 30-nm-thick chromium electrode layer was deposited on the wafer surface using electron beam evaporation (EBE) or ion beam etching (IBE). The fabricated periodic electrode structures exhibited no broken lines or burrs, with clearly defined features and uniform quality across the entire wafer.

⑶ **Poling:** A programmable high-voltage pulse poling system was set up to pole the electrode-patterned wafer. To reduce the coercive field of the material, the wafer was placed in the oil bath and poled at elevated temperature of 120 °C. High-voltage pulses with durations on the order of hundreds of milliseconds were applied. By controlling the amplitude and duration of the high-voltage pulses, the domain inversion duty cycle was regulated to approach 50%.

⑷ **Etching:** After obtaining the periodically poled domain structure, the surface chromium electrodes were removed. Inductively Coupled Plasma (ICP) etching was performed on the domain-inverted regions to a depth of 7 μm. In each of the three poling period regions, five waveguides with widths varying from 7 μm to 11 μm were fabricated, with an etch sidewall angle of 70°. After removing surface redeposits, waveguide structures with propagation losses below 1.6 dB/cm were obtained.

⑸ **Dicing and Polishing:** The entire wafer was diced to obtain chip arrays of the desired dimensions, with every five chips grouped as a unit, followed by end-face polishing of the chips. Before polishing, a protective layer (photoresist or silicon oxide) was applied to the waveguide surface to prevent stress-induced delamination of the film, which could render the chips nonfunctional. After polishing, the chips were diced again to yield the final individual small chips.

⑹ **Coating:** Using a custom-designed chip holder, the chips were clamped so that only the end facets to be coated remained exposed. The loaded fixtures were placed into a coating machine for double-side anti-reflection (AR) coating. The coating specification was S1&S2 AR: 1500-1620/750-810 nm. The coating results were tested using a PE-lambda 1050+ spectrophotometer, and the reflectivity was confirmed to be below 0.5% over the specified wavelength ranges.

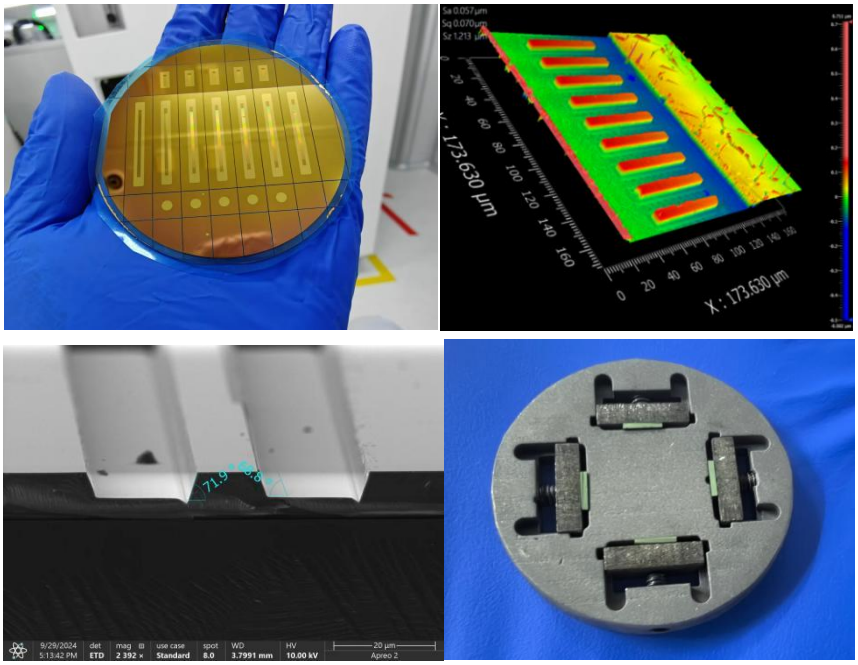


Figure 4 PPLN waveguide chip: (a) photograph of the electrodes, (b) etched surface image after poling, (c) SEM image of the ridge waveguide after etching, (d) photograph of the coating fixture.

3.2 780 nm Femtosecond SHG Chip Testing System

⑴ Insertion loss test

After chip fabrication, the insertion loss (IL) of the waveguides was tested using a broadband femtosecond fundamental-wave source. Waveguides with lower insertion loss generally corresponded to higher SHG efficiency, serving as a reference for waveguide selection prior to SHG testing. A photograph of a fabricated chip is shown in figure 5.

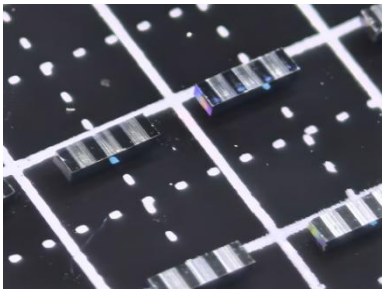


Figure 5 Photograph of a 1 mm long PPLN waveguide chip for 780 nm femtosecond laser

A continuous-wave (CW) light source with a wavelength of 1560 nm and an output power of 10 mW was selected. Under this power level, the SHG conversion efficiency is below 1%, and the frequency-doubled component in the output can be considered negligible. Therefore, the insertion loss of the chip can be determined by monitoring

the variation in the output power of the 1560 nm fundamental light before and after inserting the chip under test. The experimental setup is shown in the figure below. On a semi-automatic alignment stage, the input and output fibers were first aligned, and the output fundamental-wave power was recorded as P_0. The chip under test was then placed between the input and output fibers; the fibers were realigned to the chip end faces, and the optical path was optimized to maximize the output fundamental-wave power, with the corresponding power value recorded as P_1. The insertion loss can be calculated using the following formula:

$$IL=-log_{10}(\frac{P_1}{P_0}) \tag{7}$$

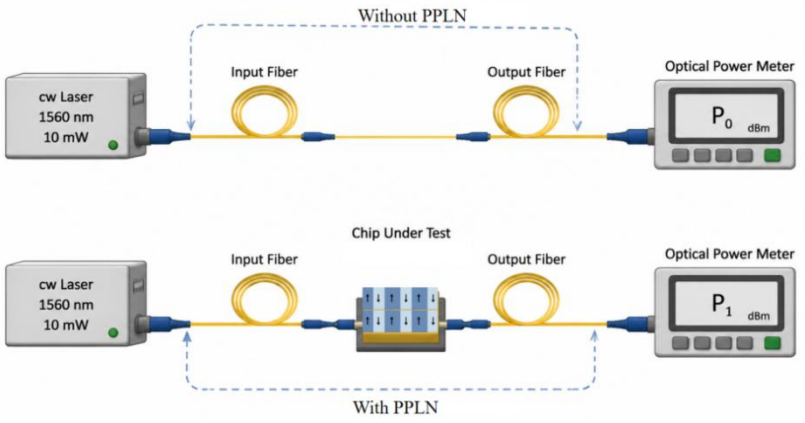


Figure 6 Experimental Setup for Insertion Loss Measurement of Femtosecond SHG Chips

Ten PPLN chips from the same wafer batch were selected, and the insertion loss (IL) of the waveguides in channels A, B, and C on each chip was measured individually. Each channel was measured three times and the results were averaged, with the lowest IL value recorded for each chip. The test results are summarized in the table below. As shown in the table, the insertion loss of the best-performing channel in all ten chips is below 2 dB, indicating that the waveguide fabrication process exhibits good uniformity and repeatability. Taking into account both insertion loss and poling period matching, channel B5 of chip A03-10Z-1mm-05 (IL = 1.2 dB) was selected as the candidate waveguide for subsequent femtosecond SHG efficiency testing.

Table 2 Results of waveguide insertion loss

Chip Number	Channel	Insertion loss / dB
A03-10Z-1mm-01	B5	1.9
A03-10Z-1mm-02	B1	1.9
A03-10Z-1mm-03	B3	1.4
A03-10Z-1mm-04	C3	1.9
A03-10Z-1mm-05	B5	1.2
A03-10Z-1mm-06	B4	1.3
A03-10Z-1mm-07	B1	1.3
A03-10Z-1mm-08	B2	1.4
A03-10Z-1mm-09	B4	1.3
A03-10Z-1mm-10	B2	1.5

(2) SHG efficiency test

Experiments were first conducted to characterize the SHG performance of the PPLN chip. The experimental setup was shown in figure 7. The fundamental laser had a repetition rate of 80 MHz, an average output power of 43.1 mW, and a femtosecond pulse duration of 50 fs. After propagating through a 30-mm-long polarization-maintaining (PM) fiber, the polarization direction of the fiber was aligned parallel to the +Z axis of the chip by adjusting the fiber angular orientation (FA). The fiber was then coupled and aligned to the waveguide end facet of the chip, with the optical power measured at the FA position being 40.0 mW. A micro-lens with an anti-reflection (AR) coating centered at 780 nm was employed, having a transmittance of 98%. The power meter was responsive only to the 780 nm band and not to the fundamental-wave band. The measured second-harmonic power was 17.2 mW, corresponding to an absolute SHG conversion efficiency of 43%.

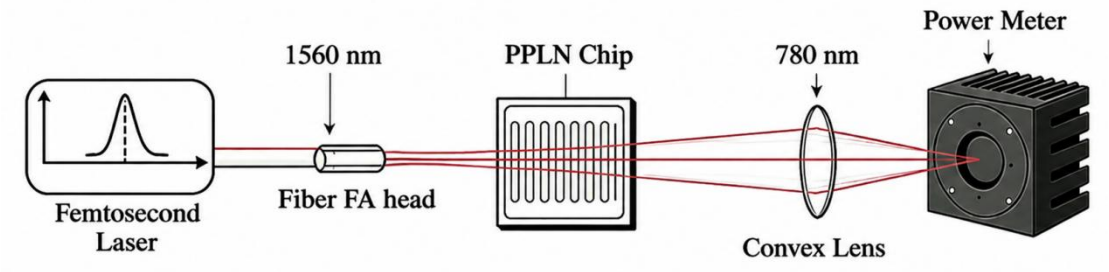


Figure 7 Schematic of the 780 nm femtosecond laser SHG test system

To verify the SHG performance of the 1-mm-long chip at elevated input average powers, the femtosecond laser fundamental-wave parameters were adjusted such that the average input power was 80.0 mW, with the pulse duration broadened to 100 fs at a repetition rate of 80 MHz. The measured second-harmonic power was 30.1 mW, corresponding to a conversion efficiency of 37.6%. From the comparison of these parameters, it can be seen that as the fundamental-wave power increases, the absolute second-harmonic power also increases; however, due to pulse broadening, the conversion efficiency decreases, indicating that the SHG efficiency is jointly influenced by the fundamental-wave average power, the laser pulse peak power, and the crystal length. A photograph of the chip SHG test setup is shown in figure 8. A PM1550 single-mode polarization-maintaining fiber was employed, and the chip used was the self-developed 780 nm femtosecond SHG chip. The lens was an aspheric coupling lens with an anti-reflection coating centered at 780 nm.

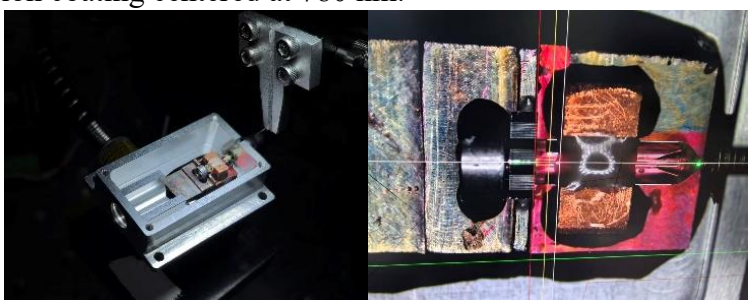


Figure 8 780 nm Femtosecond SHG Chip Performance test

A packaging structure for the femtosecond SHG chip was designed, and the

device-level packaging of the chip was subsequently completed. The chip can be configured either with fiber input and fiber output, or with fiber input and free-space output. Based on application requirements, a packaging with fiber input and free-space output was first designed, as shown in figure9. A reflective dichroic mirror was inserted between the collimating lens and the focusing lens to filter out the fundamental-wave component from the output laser.

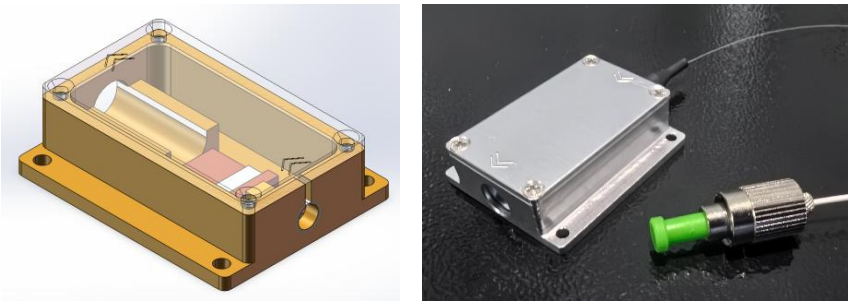


Figure 9 780 nm Femtosecond SHG Chip Packaging Design and Device Photograph

The chip was bonded to the heat sink using conductive silver epoxy, while the collimating lens was attached to the heat sink with UV-curable adhesive. The thermal curing was performed at 150℃ for 2 h. The lens and dichroic mirror were bonded using a thermally cured adhesive. After all components were bonded, the device was subjected to aging to relieve residual stresses from the bonding process. Typically, the device was baked in a temperature chamber at 85 °C for 12 h; for devices with stringent environmental requirements, a thermal cycling protocol of −20 °C to 85 °C with a 2-h cycle period was applied for a total of 12 h.

In the 780 nm femtosecond SHG device, the fundamental wave is input via an optical fiber and coupled into the femtosecond SHG chip, with two lenses providing either collimated or focused free-space output. The device is plug-and-play, robust and durable, demonstrating good environmental adaptability. An optical spectrum analyzer (OSA) was used to measure the spectra of both the fundamental wave and the second-harmonic wave, and the measurement results are shown in figure 10.

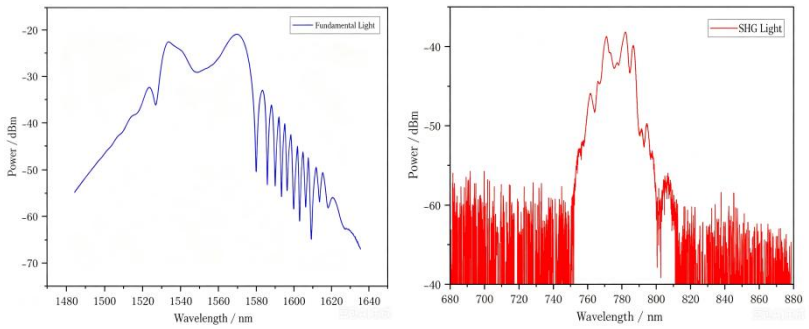


Figure 10 Spectral response curves of the femtosecond laser fundamental and second harmonic lights

The figures show that the second harmonic wavelength is centered around 780 nm ± 15 nm, while the fundamental wavelength is centered around 1560 nm ± 30 nm. The spectral width of the second harmonic is approximately half that of the fundamental.

The long-term output power stability of the second harmonic is also a critical metric for evaluating device performance, particularly under conditions of higher second-harmonic output power. For this purpose, the fundamental-wave average input

power was set to 80 mW, yielding a second-harmonic average output power of 30.1 mW. The power stability was measured as RMS < 0.2% over a 2-hour period. The femtosecond waveguide SHG device demonstrated strong tolerance to high peak powers as well as reliable long-term operational stability. The test results are shown in figure 11.

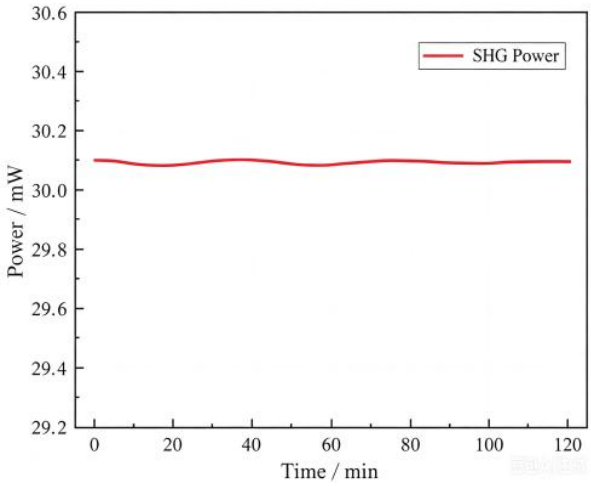


Figure 11 Power stability of the 780 nm femtosecond laser

The SHG conversion efficiency of ultrashort-pulse lasers is jointly determined by the pump source parameters and the nonlinear crystal parameters. From both simulation and experimental perspectives, the choice of crystal length is related to the pump bandwidth: the crystal must be sufficiently long to provide high gain, while its acceptance bandwidth should ideally be no narrower than the pump bandwidth. When the pump bandwidth significantly exceeds the crystal acceptance bandwidth, the pump frequency components outside the acceptance bandwidth can still contribute to the conversion efficiency enhancement via sum-frequency generation (SFG), which essentially compresses the broadband pump light into narrowband second-harmonic output. As a general guideline, a waveguide length of 0.5–1 mm is recommended for pulse durations of 50–200 fs; 1–3 mm for 200–500 fs; 3–10 mm for 0.5–3 ps; and 10–40 mm for nanosecond and continuous-wave (CW) laser systems. The corresponding SHG conversion efficiency can reach 40%–60%. Furthermore, waveguides shorter than 1 mm exhibit a very broad temperature acceptance bandwidth, enabling efficient 780 nm femtosecond laser output at room temperature without active temperature control.

4 Conclusion

This paper presents the development process of PPLN waveguides for a 780 nm femtosecond laser. Starting from phase-matching techniques, the principles and simulation results of femtosecond laser second-harmonic generation are introduced, leading to the conclusion that the SHG conversion efficiency is subject to a non-monotonic modulation by the crystal length. Through chip design and wafer fabrication, PPLN waveguide chips with four different lengths, 0.5 mm, 1.0 mm, 1.5 mm, and 2.0 mm, were prepared. A 780 nm femtosecond SHG test system was constructed, and under the fundamental-wave input conditions of an 80 MHz repetition rate, 40 mW average power, and a 100 fs pulse duration, a 780 nm femtosecond second-harmonic

laser with an output power of 17.2 mW was generated, achieving an absolute SHG conversion efficiency of 43%.

Declarations

The authors declare that they have no known competing financial interests or personal relationships that could have appeared to influence the work reported in this paper.

Acknowledgments

Xu Xiaohu is an engineer at Huazhong University of Science and Technology. He is currently working on nonlinear optics and integrated photonic chips, with particular emphasis on periodically poled lithium niobate (PPLN) waveguide devices for nonlinear frequency conversion. This work is funded by the National Natural Science Foundation of China. (No. 62305315, U25D8011).

References

[1] Cumpston B H, Ananthavel S P, Barlow S, et al.l.Two-photon polymerization initiators for three-dimensional optical data storage and microfabrication[J]. Nature, 1999, 398(4):51-54.

[2] Jiang X, Chen F, Yin T, et al. Generation of high-power 780 nm femtosecond pulses by an all-polarization-maintaining Er-doped fiber amplification system. Applied Optics, 2019, 58(16): 4492-4496.

[3] Roskos H G, Thomson M D, Kren M, et al.Broadband THz emission from gas plasmas induced by femtosecond optical pulses :from fundamentals to applications[J].Laser&Photonics Review,2007,1(4):349-368.

[4] Zhang Y, Hou FY, Liu T, et al. et al Generation and quantum characterization of miniaturized frequency entangled source in telecommunication band based on type-II periodically poled lithium niobate waveguide [J].Acta Physica Sinca, 2018, 67(14): 171-178.

[5] Yamakawa, K., et al. 100-TW sub-20-fs Ti: sapphire laser system operating at a 10-Hz repetition rate[J].Optics letters,1998,23 (18): 1468-1470.

[6] Wu JR, Lv ZQ, Lu X, et al. Characteristics of Second Harmonic Generation in Erbium Doped Femtosecond Fiber Lasers Based on Quasi Phase Matching[J].Chinese Journal of Lasers, 2018,45(7):0701001-1-7.

[7] Xiaogang Jiang, Feihong Chen, Taoce Yin, et al. Generation of high-power 780 nm femtosecond pulses by an all-polarization-maintaining Er-doped fiber amplification system[J],Appl. Opt. 2019,58(16):4492-4496.

[8] Franken P A, Hill A E, Peters C W, et al. Generation of Optical Harmonics [J]. Physical Review Letters, 1961, 7(4):118-119.

[9] Luo T. High power 780 nm femtosecondall polarization-maintaining fiber laserand its engineering integration [M]. Guangzhou: South China University of Technology, 2024.

[10] Huang, Zhangchao, et al.Femtosecond second-harmonic generation in periodically poled lithium niobate waveguides written by femtosecond laser pulses [J].Optics letters,2010,35(6): 877-879.
[11] ZHENG, Zheng, et al. Femtosecond second-harmonic generation in periodically poled lithium niobate waveguides with simultaneous strong pump depletion and group-velocity walk-off[J]. Journal of the Optical Society of America B, 2002, 19(4): 839-848.